ACS OMEGA

http://pubs.acs.org/journal/acsodf

Article

Kinetic Study of Copyrolysis of the Green Microalgae *Botryococcus braunii* and Victorian Brown Coal by Thermogravimetric Analysis

R. R. Dirgarini Julia Nurlianti Subagyono,* Wardina Masdalifa, Siti Aminah, Rudy Agung Nugroho, Mamun Mollah, Veliyana Londong Allo, and Rahmat Gunawan

Cite This: *ACS Omega* 2021, 6, 32032−32042

Read Online

ACCESS | Metrics & More | Article Recommendations

ABSTRACT: The copyrolysis of the green microalgae *Botryococcus braunii* and Victorian brown coal was studied by thermogravimetric analysis using the Kissinger−Akahira−Sunose (KAS), Flynn−Wall−Ozawa (FWO), and Friedman methods. This research aims to study the synergistic effect of mixing *B. braunii* and Victorian brown coal in pyrolysis reactions on the kinetic parameter using thermogravimetric analysis. Copyrolysis was carried out at four heating rates, 10, 15, 20, and 25 °C/min. The copyrolysis reaction of *B. braunii* and Victorian brown coal occurred from 155.79 to 545.27 °C; this temperature range was lower than that for the pyrolysis of only *B. braunii* under the same conditions. However, mixing the two samples increased the thermal decomposition temperature for each conversion value (α), as well as the average activation energy, due to the presence of compounds that require high temperatures to undergo pyrolysis in the Victorian brown coal. The average activation energies of the copyrolysis reaction of *B. braunii* and Victorian brown coal determined using the KAS, FWO, and Friedman methods were 195.20 ± 17.40, 195.60 ± 17.70, and 225.93 ± 32.39 kJ/mol, respectively.

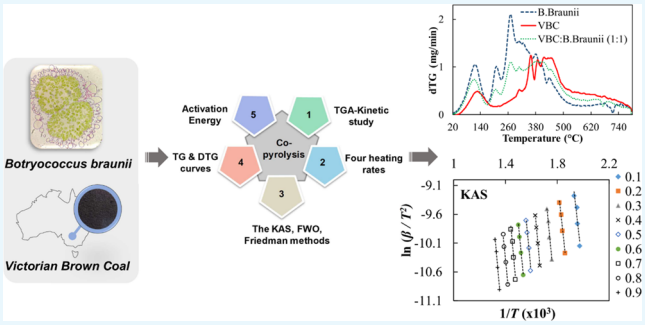

1. INTRODUCTION

Biomass is a renewable energy source and is considered environmentally friendly. However, when compared to conventional energy sources such as coal, biomass has a higher oxygen content, higher moisture content, lower ash melting temperature, and lower calorific value.[1] Combining coal and biomass is one solution to maintain energy content through methods such as cofiring,[2,3] cogasification,[4−6] and copyrolysis.[7−11] In addition, the combination of biomass and fossil fuels, such as coal, provides many advantages. The addition of coal to biomass can increase the energy density of the feedstock and reduce fluctuations in the supply of biomass. In contrast, adding biomass to coal can reduce pollutants (such as SO_x and NO_x) as well as reduce fossil CO_2 emissions (i.e., the greenhouse effect). Biomass can increase the reactivity of coal during thermal processes (i.e., in pyrolysis and gasification) because biomass contains a larger amount of hydrogen and other species with catalytic activity.[1]

Microalgae are a potential biomass to be combined with coal for energy production. Microalgae have many advantages over terrestrial biomass; they are not edible, have a faster growth rate and higher productivity, much higher oil production, the ability to absorb CO_2 in the atmosphere, and the ability to grow on uncultivated land, contaminated water, and under variable climatic conditions.[12−15] However, for large-scale energy production from microalgae, several aspects need to be considered, such as the production costs and the availability of water, CO_2, sunlight, and flat land.[14,16]

In this paper, the copyrolysis of the green microalgae, *Botryococcus braunii*, and Victorian brown coal (VBC) is studied by thermogravimetric analysis (TGA). *B. braunii* is a unicellular photosynthetic species of microalgae belonging to the *Chlorophyceae* (Chlorophyta). These microalgal colonies are widely distributed in fresh and brackish water. *B. braunii* is considered a potential source of renewable fuels because it can produce large amounts of hydrocarbons through a thermal conversion process.[17−19] The hydrocarbons produced by *B. braunii* in the form of lipids can reach up to 75% of the dry mass of the algae, depending on the growing conditions.[20,21] The hydrocarbons produced by *B. braunii* include *n*-alkadienes, trienes, botryococcenes, triterpenoids, tetraterpenoids, and lycopadiene.[22] The coal used is VBC, a low-quality coal with unique physical and chemical properties. Almost all of the

Received: September 1, 2021
Accepted: November 10, 2021
Published: November 18, 2021

characteristics of VBC are unique compared to other solid fuels such as biomass, peat, bituminous coal, and anthracite.[23]

During pyrolysis, microalgae will form many alkyl radicals and increase or decrease hydrogen radicals from alkyl radicals to produce *n*-alkanes or *n*-olefins, respectively. Thus, microalgal pyrolysis oil has a higher hydrocarbon content and lower oxygen content. The copyrolysis of microalgae and coal can increase the yield and tar quality under mild copyrolysis conditions.[24] Although *B. braunii* has been studied for energy production via a thermochemical conversion process,[17,25] the use of this microalgal species with a low rank coal, such as VBC, in the copyrolysis process has not been explored in depth. VBC is abundantly available, inexpensive, and has a low mineral content of impurities, and it has the potential, therefore, to be used as a raw material in the pyrolysis process.[26] Furthermore, few studies have investigated the use of VBC for copyrolysis with microalgae.[27] Hence, the kinetics of copyrolysis of *B. braunii* and VBC are worth studying.

TGA can be used to study and understand the kinetics of pyrolysis and copyrolysis of biomass, such as microalgae, with coal.[11,24,28−33] There are many methods for analyzing kinetic data from TGA, but the two most commonly applied types are "model-fitting"[34] and "model-free".[35] The model-free approach is used more commonly in kinetic studies due to the inability of the model-fitting method to adequately characterize nonisothermal data. The model-free approach is preferred based on its simplicity and avoidance of errors related to the kinetic model choice. The model-free method also allows the better fitting of thermogravimetric curves than the model-fitting method.[36] This method, however, requires collecting several kinetic curves to perform the analysis. The determination of reaction rates collected at different heating rates can be achieved at the same conversion value, making it possible to calculate the activation energy at each conversion point.[37] The kinetic of *B. braunii* pyrolysis have been studied previously using both model-free and model-fitting methods.[38,39]

In this paper, we report the kinetic analysis of the copyrolysis of *B. braunii* and VBC using model-free kinetic methods, specifically the Kissinger−Akahira−Sunose (KAS),[40] Flynn−Wall−Ozawa (FWO),[41] and Friedman[42] methods. These three methods were chosen based on several reasons: (1) these three kinetic models are the most common methods used to determine the activation energy value of biomass using the pyrolysis method, (2) they are easier to use to determine the value of activation energy, and (3) they have better accuracy than other model-free methods.[43] These three data processing methods were used to compare the activation energy values of the differential isoconversional (Friedman) method and the integral isoconversional (FWO and KAS) methods. The activation energy of the copyrolysis reaction and the copyrolysis temperature range of microalgae and coal were determined.

2. RESULTS AND DISCUSSION

2.1. Characterization of *B. braunii*. The characterization of the microalgal samples determines the water content, ash content, and chemical composition of *B. braunii*, which were used as supporting data to explain the pyrolysis process. The physical and chemical properties of *B. braunii* are presented in Table 1. The moisture content of the freeze-dried sample of *B. braunii* was 5.01 ± 0.42 wt %. For an effective combustion process, the maximum moisture content in biomass should be around 5%.[44] The high water content of the biomass can reduce the efficiency of thermochemical conversions, such as gasification, by reducing the heating value of the biomass, causing incomplete combustion. The water content affects the net calorific value, the combustion efficiency, and the combustion temperature because some of the energy will be used to evaporate the water contained in the sample.[45] The ash content of the *B. braunii* sample (27.44 ± 1.11 wt %) indicated the amount of inorganic minerals and other elements present in the microalgae. High ash content can cause environmental pollution due to increased dust emissions and increase the possibility of slag formation and deposition in the furnace.[45]

Table 1. Physical and Chemical Properties of *B. braunii*

properties	values
water content (wt %)	5.01 ± 0.42
ash content (wt %)	27.44 ± 1.11
protein content (wt %)	14.8 ± 0.1
chlorophyll *a* (mg/L)	255.30 ± 3.19
chlorophyll *b* (mg/L)	392.85 ± 5.34
total chlorophyll (mg/L)	647.63 ± 2.15
fatty acid composition (%)	
myristoleic acid ($C_{14:1}$)	0.92
palmitoleic acid ($C_{16:1}$)	34.98
margaric acid ($C_{17:0}$)	0.21
linoleic acid ($C_{18:2n6c}$)	4.46
linolelaidic acid ($C_{18:2n6t}$)	45.85
γ-linolenic acid ($C_{18:3n6}$)	13.58
total saturated fatty acids	0.21
total unsaturated fatty acids	99.79

The protein and chlorophyll contents of *B. braunii* are presented in Table 1. During the thermal conversion process, the nitrogen in the protein and the chlorophyll in *B. braunii* can be released as volatile compounds that contain nitrogen, such as ammonia and NO_x precursors, which can become pollutants.[46,47] In the pyrolysis process, the reaction between fatty acids and ammonia produces alkyl nitriles,[48,49] an undesirable product in the fuel because of the potential to reduce catalytic activity in the upgrading process.[50,51]

Gas chromatographic analysis showed that *B. braunii* contained various types of fatty acids (Table 1). Linolelaidic acid (45.85%) and palmitoleic acid (34.98%) were the unsaturated fatty acids with the highest percentage in the algal sample. A high percentage of unsaturated fatty acids in microalgae can affect the active temperature of pyrolysis: the higher the unsaturated fatty acid content, the higher the temperature required for thermal degradation.[52]

2.2. Thermogravimetric Analyses. The thermogravimetry (TG) curve and the first derivative of the TG curve (the dTG curve) of the pyrolysis of the microalgae *B. braunii* at different heating rates are presented in Figure 1a,b. The curves are divided into three regions that indicate the three stages during the experiments (Table 2). The first stage was the evaporation of moisture and low-boiling point organic compounds at ≤156 °C (depending on the heating rates). In addition, during this stage, the decomposition of chlorophyll may also have occurred at 80−110 °C because chlorophyll is an unstable compound and may be easily degraded at 80−145 °C.[53] However, chlorophyll decomposition at this stage did not produce compounds, such as phytane and pristane, which are pyrolysis products of chlorophyll in microalgae.[48] In the second stage, active pyrolysis occurred from ±156 to 557 °C (depending on the heating rates). In active pyrolysis, thermal

https://doi.org/10.1021/acsomega.1c04818
ACS Omega 2021, 6, 32032−32042

Table 2. Stages during the Pyrolysis of *B. braunii* and Copyrolysis of *B. braunii* and VBC at Different Heating Rates

	pyrolysis		copyrolysis	
stage	temperature (°C)	mass loss (%)	temperature (°C)	mass loss (%)
evaporation of moisture and low-boiling point compounds	≤156	7−10	≤156	5−9
active pyrolysis	±156−557	52−54	±156−545	46−48
passive pyrolysis	±557−800	8−10	±545−800	10−13

decomposition, depolymerization, decarboxylation, and cracking of carbohydrates, proteins, chlorophyll, and lipid compounds in microalgae occurred. Carbohydrates decomposed at 200−300 °C and proteins decomposed at 280−400 °C. The lipids in the microalgae were thermally degraded at 270−550 °C, a range similar to that reported by Chen et al.[54] In the dTG curve (Figure 1b), two prominent peaks were observed during active pyrolysis, one weak peak and one sharp peak indicating the thermal degradation of the chemical constituents in the sample. The first, weaker peak (150−250 °C) represented the decomposition of the proteins and carbohydrates, while the second, sharper peak (280−350 °C) represented the decomposition of the lipids.[55] In the third stage, passive pyrolysis was observed when the dTG graph started at ±526-557 °C (depending on the heating rates), which was indicated by flat curves. In passive pyrolysis, compound decomposition occurs due to gasification, as well as the formation of nonvolatile carbon compounds that evaporate to form gaseous CO and CO_2 at high temperatures.[55]

Figure 1c,d presents the TG and dTG curves of the copyrolysis of *B. braunii* and VBC under a nitrogen atmosphere at different heating rates. Similar to the pyrolysis experiments, there were three main steps observed in the TG and dTG curves (Table 4). The first stage, also referred to as the drying stage, involved the evaporation of water or moisture and light volatile compounds present in the mixture of *B. braunii* and VBC. In this study, the first stage occurred at ≤156 °C (depending on the heating rates), where the evaporation of water and light volatile compounds occurred at 80−150 °C. It is important to note that the temperature of the first stage in the copyrolysis of *B. braunii* and VBC was similar to that of the pyrolysis of *B. braunii*; this was possible because both samples have been dried to have a similar water content. This temperature range agreed with the study of Chen et al.,[54] where a similar volatilization process occurred between 25 and 168−178 °C. Other studies of the copyrolysis of coal and biomass also found that the evaporation temperatures of water and light volatiles occurred at <200 °C.[8]

Similar to the pyrolysis experiments of *B. braunii*, the second stage (156−545 °C) included active copyrolysis, which involved the largest mass reduction (46−48%), due to the decomposition of carbohydrates, proteins (250−280 °C), chlorophyll, and lipids (380−480 °C) from microalgae as well as lignin- or cellulose-derived materials, phenolic aromatic carbons, substituted aliphatic carbons, and other oxygen-containing compounds in VBC. These compounds underwent depolymerization, decarboxylation, and cracking processes releasing volatile molecules, H_2O, CO_2, and CO.[8,11,24,39,56−59]

The third stage is known as the endothermic decomposition of lignin-derived materials and carbonaceous materials, in

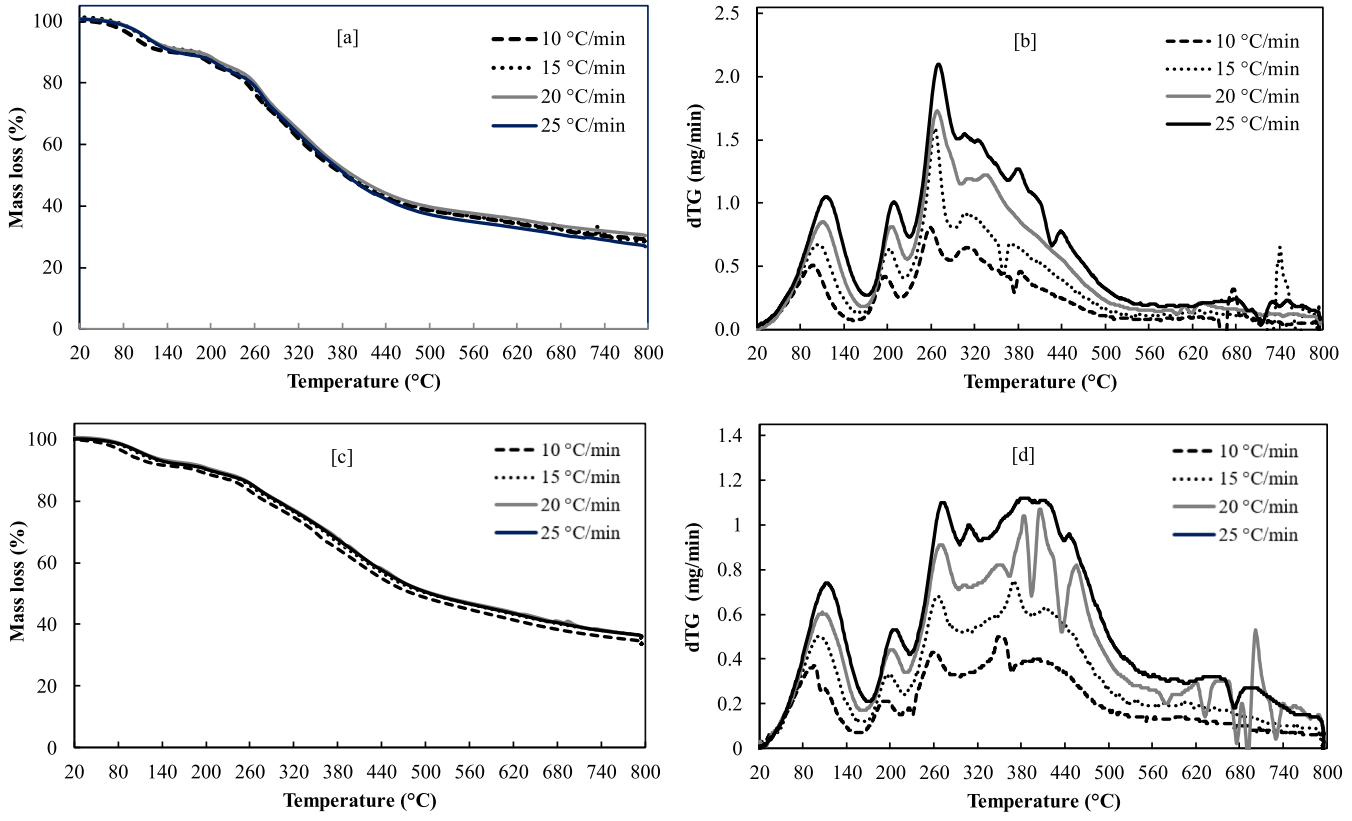

Figure 1. TG (a) and dTG (b) curves of pyrolysis of *B. braunii* and TG (c) and dTG (d) curves of copyrolysis of *B. braunii* and VBC at different heating rates.

https://doi.org/10.1021/acsomega.1c04818
ACS Omega 2021, 6, 32032−32042

which carbon residues decompose slowly.[54,60] This stage occurred in the temperature range of 545−800 °C and caused a mass reduction of 10−13%, which lasted until the remaining mass was char. One study has also shown that the interaction between coal and biomass during copyrolysis demonstrates an inhibitory effect on thermal decomposition and release of volatiles, resulting in a higher char yield than expected.[57]

From the dTG curves of the pyrolysis and copyrolysis experiments in this study (Figure 1b,d), it is clear that there was a shift in the pyrolytic curve to a higher temperature with an increase in the heating rate. The results are in good agreement with a similar study by Ali et al.[38] Heating of the samples occurred more gradually at lower heating rates, enabling better and more effective heat transfer to the particles.[61] The thermal decomposition proceeds at a slower rate at higher heating rates due to inefficient heat transfer.[62] Increasing the heating rate can release more volatile matter, resulting in less pyrolysis residue.

In this study, the active pyrolysis and copyrolysis temperatures at different heating rates were determined from the TG and dTG curves and are presented in Table 3. The results showed that an increase in the heating rate in the pyrolysis or copyrolysis process increased the temperature range of the active pyrolysis (higher $T_{initial}$ and T_{final}). The increase in the active pyrolysis temperature may be due to the rapid increase of the temperature difference between the particle surface and core, resulting in a gradient that supported the heat transfer.[39] An increase in the heating rate can cause the ambient temperature to pass through a wider interval per unit time. That is, at the same initial temperature, there was an increase in the average temperature of the sample per unit time, which resulted in maximum decomposition.[57] Table 3 also shows that the temperature range of active pyrolysis for the copyrolysis experiments was higher than that of the pyrolysis experiments. A possible explanation of this result is discussed later.

Table 3. Temperature Range of Pyrolysis of *B. braunii* and Temperature Range of Copyrolysis of *B. braunii* and VBC at Different Heating Rates

	pyrolysis of *B. braunii*		pyrolysis of VBC		copyrolysis of *B. braunii* and VBC	
heating rate (°C/min)	$T_{initial}$ (°C)	T_{final} (°C)	$T_{initial}$ (°C)	T_{final} (°C)	$T_{initial}$ (°C)	T_{final} (°C)
10	156.20	526.48			155.79	521.21
15	163.79	535.89			160.94	533.53
20	165.85	543.00			161.70	537.96
25	171.26	557.24	210.76	542.39	169.99	545.27

In order to investigate the synergistic effect of *B. braunii* and VBC during copyrolysis, the TG and dTG curves for the pyrolysis of *B. braunii*, VBC, and a mixture of *B. braunii* and VBC under the same conditions were measured (Figure 2). Figure 2 shows that the decomposition of pure VBC occurred at a higher temperature range than pure microalgae (Table 3). The mixing of microalgae and coal reduced the temperature range of active pyrolysis. According to Wu et al.,[24] the mechanism of the synergistic effect has mainly been associated with the transfer of hydrogen radicals from the biomass. Depolymerization and dehydration reactions of proteins and lipids in the biomass can produce hydrogen radicals, which resulted in the faster formation of volatile compounds[24] other than charcoal products, where hydrogen radicals, together with metals present in the crystal structure of the coal and microalgae, may act as catalysts to promote the demethoxylation of aromatic compounds. As a result, a synergistic effect occurred because some materials tend to decompose faster at lower temperatures than expected.[11,24]

2.3. Kinetic Study. The thermal decomposition temperatures at different conversion values (or conversion rates) and heating rates for the pyrolysis and copyrolysis experiments were determined before the activation energies were calculated (Table 4). Table 4 shows that increased heating rates resulted in an increased thermal decomposition temperature of *B. braunii* at the same conversion rate. According to Chen et al.,[54] as the heating rate increased, the reaction rate also increased to reach a certain environmental temperature, so that the time needed for the samples (e.g., biomass) to degrade decreased. This change has been attributed to an increase in the heat transfer boundary effect, which caused a temperature gradient within each particle in the sample.[63]

The Arrhenius plots of the pyrolysis of *B. braunii* at different conversion rates calculated by the Friedman, KAS, and FWO methods are presented in Figure 3. The activation energy was determined at each conversion rate based on the slope of the Arrhenius plots. The activation energies of the pyrolysis of *B. braunii* were different for each conversion rate (Table 4). The pyrolysis of *B. braunii* was a gradual process, and the reaction mechanism changed with increased temperature. Therefore, the activation energy also changed as the reaction proceeded. The average value of the activation energy obtained using the KAS method (183.95 ± 20.32 kJ/mol) was not greatly

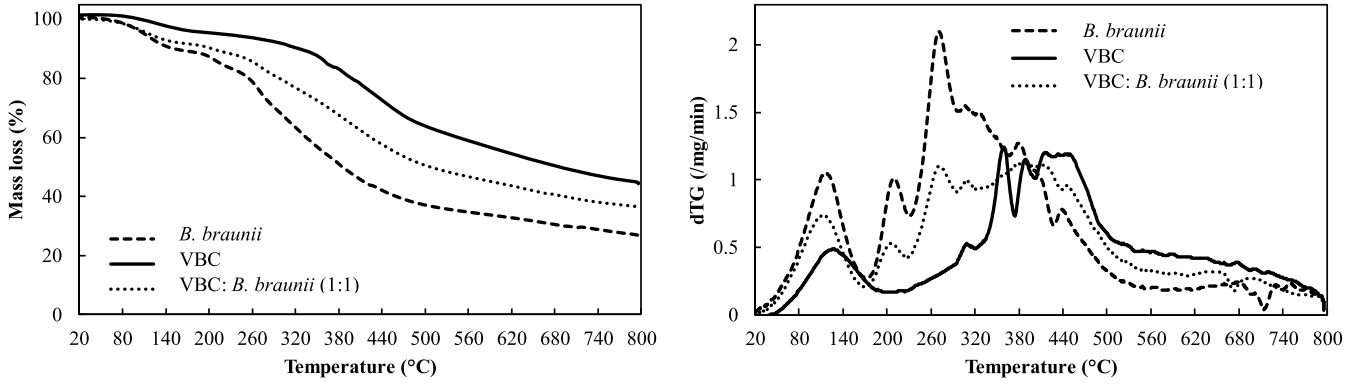

Figure 2. TG (left) and dTG (right) curves of pyrolysis of *B. braunii* or VBC and copyrolysis of *B. braunii* and VBC (heating rate = 25 °C/min).

https://doi.org/10.1021/acsomega.1c04818
ACS Omega 2021, 6, 32032−32042

Table 4. Decomposition Temperatures of Pyrolysis of *B. braunii* and Copyrolysis of *B. braunii* and VBC at Different Conversion Values

		decomposition temperature (°C)			
	conversion rate (α)	10 °C/min	15 °C/min	20 °C/min	25 °C/min
pyrolysis of *B. braunii*	0.1	217.52	220.69	225.18	227.79
	0.2	251.16	255.53	259.80	262.59
	0.3	268.10	269.78	276.49	279.26
	0.4	291.10	291.45	297.90	301.70
	0.5	313.40	315.13	320.97	325.41
	0.6	336.41	338.89	345.74	350.46
	0.7	363.73	369.70	371.59	380.11
	0.8	396.25	400.30	403.30	410.68
	0.9	438.28	444.52	447.44	457.34
copyrolysis of *B. braunii* and VBC	0.1	233.27	237.75	239.02	245.05
	0.2	264.54	270.16	272.68	277.22
	0.3	295.48	301.98	304.01	308.16
	0.4	326.93	332.62	336.71	340.38
	0.5	353.84	358.52	364.78	367.71
	0.6	377.83	384.82	389.16	393.88
	0.7	404.44	410.34	414.04	420.89
	0.8	432.44	439.36	447.40	449.12
	0.9	465.95	473.60	478.52	484.80

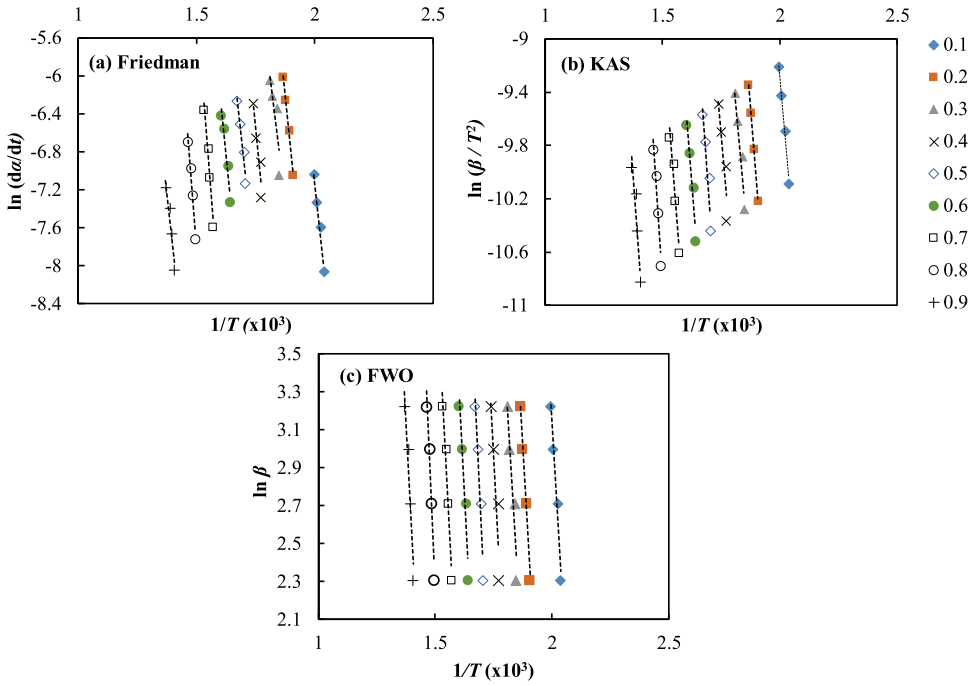

Figure 3. Arrhenius plots of pyrolysis of *B. braunii* at different conversion rates by the Friedman (a), KAS (b), and FWO (c) methods.

different from that obtained using the FWO method (185.15 ± 18.90 kJ/mol). However, the activation energy obtained using the Friedman method was 215.42 ± 32.39 kJ/mol (Table 4).

There was a significant difference between the E_a−α dependence indicated by the KAS and FWO methods and that determined by the Friedman method. This variation may have been due to the assumption, implicit in integral methods such as KAS and FWO, that E_a is independent of α,[64] whereas the Friedman calculations, which do not require this assumption, indicated that this was not the case. Therefore, in drawing conclusions regarding E_a, the Friedman results must be given increased weight. However, it should be noted that a differential method, such as Friedman's, is more subject to random error, as discussed later in this paper.

Calculations using the FWO, KAS, and Friedman methods showed the same pattern for the activation energy when the conversion rate increased. For example, at $0.3 \leq \alpha \leq 0.4$, there was an increase in the value of the activation energy, namely, 167.54−180.35 kJ/mol for the FWO method, 167.09−180.20 kJ/mol for the KAS method, and 172.37−202.62 kJ/mol for the Friedman method. This trend may be due to the breakdown of carbohydrates and proteins in the microalgal sample. The decomposition of carbohydrates and proteins occurred in a temperature range of 225−300 and 300−400 °C, respectively.[62] In this study, the decomposition temperature

https://doi.org/10.1021/acsomega.1c04818
ACS Omega 2021, 6, 32032−32042

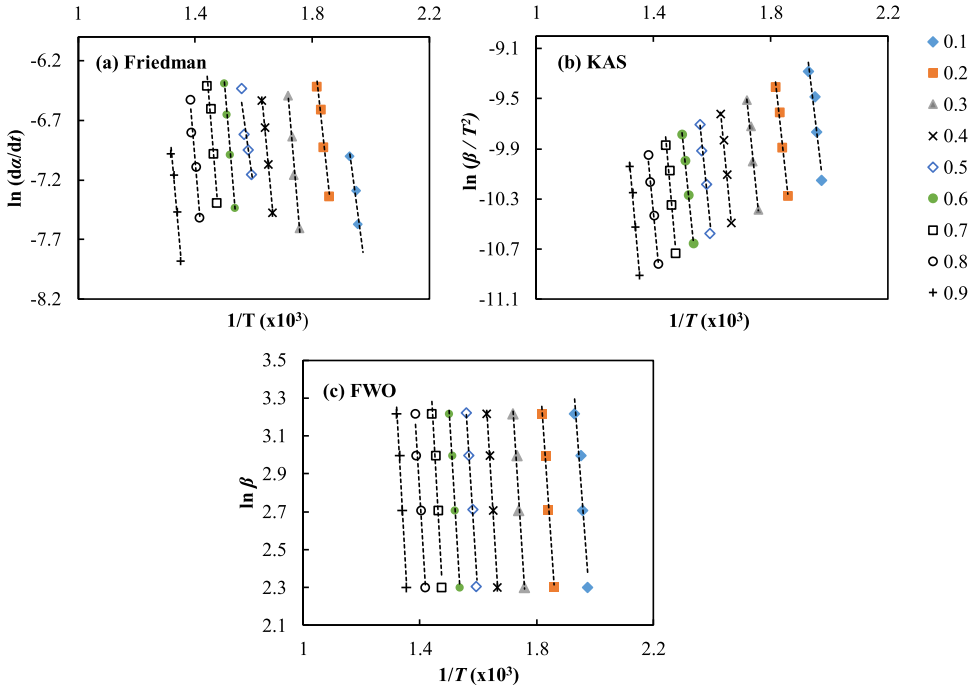

Figure 4. Arrhenius plots of copyrolysis of *B. braunii* and VBC at different conversion rates by the Friedman (a), KAS (b), and FWO (c) methods.

Table 5. Activation Energy (E_a) of Pyrolysis of *B. braunii* and Copyrolysis of *B. braunii* and VBC at Different Conversion Rates Based on the KAS, FWO, and Friedman Methods[a]

	KAS		FWO		Friedman	
conversion (α)	E_a (kJ/mol)	R^2	E_a (kJ/mol)	R^2	E_a (kJ/mol)	R^2
Pyrolysis of *B. braunii*						
0.1	166.55	0.9781	166.21	0.9801	190.92	0.9676
0.2	175.48	0.9956	175.25	0.9960	208.91	0.9941
0.3	167.09	0.9018	167.54	0.9108	172.37	0.7026
0.4	180.20	0.8301	180.35	0.8441	202.62	0.8753
0.5	189.77	0.8981	189.82	0.9070	192.55	0.9383
0.6	177.37	0.9187	178.42	0.9268	195.27	0.9264
0.7	182.47	0.9028	183.71	0.9125	260.04	0.9578
0.8	224.87	0.9035	224.53	0.9117	264.04	0.9239
0.9	193.85	0.9030	195.75	0.9131	196.18	0.9183
average	183.95 ± 20.32		185.15 ± 18.90		215.42 ± 32.39	
Copyrolysis of *B. braunii* and VBC						
0.1	161.69	0.9082	161.86	0.9165	152.74	0.8847
0.2	173.50	0.9823	173.59	0.9840	184.46	0.9743
0.3	193.78	0.9771	193.36	0.9792	244.06	0.9806
0.4	199.65	0.9992	199.45	0.9992	215.57	0.9992
0.5	199.79	0.9823	200.01	0.9840	152.39	0.8812
0.6	198.11	0.9972	198.80	0.9975	239.58	0.9972
0.7	209.34	0.9625	209.91	0.9662	240.54	0.9503
0.8	203.07	0.9732	204.40	0.9760	228.73	0.9639
0.9	217.92	0.9909	219.06	0.9919	228.59	0.9816
average	195.20 ± 17.40		195.60 ± 17.70		225.93 ± 20.70	

[a]The average activation energy values were calculated from the Arrhenius plots with $R^2 > 0.9$.

was 260−280 °C when α = 0.3 and 300 °C when α = 0.4 (Table 3). The highest activation energy for the three kinetic methods was at a conversion rate of 0.8 (temperature range 390−420 °C); this temperature range was associated with the thermal degradation of lipids in *B. braunii*, which indicated that the thermal degradation of lipids required higher activation energy than proteins and carbohydrates. A similar study by Ali et al.[38] has also found that lipids had high enough thermal stability and degraded in the temperature range of 300−500 °C, while proteins and carbohydrates had lower thermal stability and degraded in the temperature ranges of 200−300 °C and 200−350 °C, respectively.

The Arrhenius plots for the copyrolysis of *B. braunii* and VBC at different conversion rates using the Friedman, KAS, and FWO methods are presented in Figure 4. The activation energy was then determined for each conversion rate based on

https://doi.org/10.1021/acsomega.1c04818
ACS Omega 2021, 6, 32032−32042

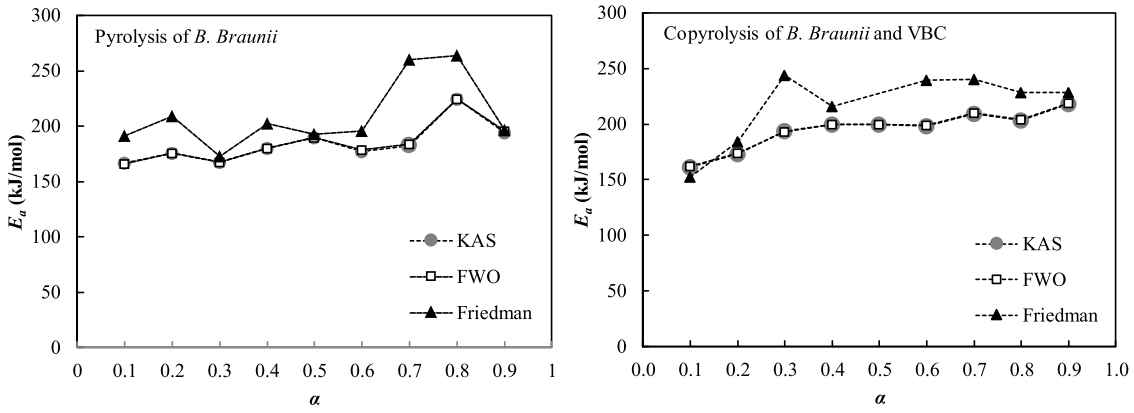

Figure 5. Energy activation values of pyrolysis of *B. braunii* and copyrolysis of *B. braunii* and VBC calculated by KAS, FWO, and Friedman methods.

the slope of the Arrhenius plots. Similar to the pyrolysis experiments, the activation energy of the copyrolysis of *B. braunii* and VBC generally increased with the conversion rate, except for those determined by the Friedman method (Table 5). One of the limitations of the Friedman method is its sensitivity to noise, which can be caused by the experimental errors and intrinsic inaccuracies, especially for nonisothermal kinetic data obtained by TGA. As a result, inaccuracies in determining the temperature or reaction rate can lead to significant differences between the correct value and the calculated value, particularly when a small number of processes are considered.[65]

The KAS and FWO methods rely on approximations to the true integral, but the approximations are not the same, and it may be that one method gives a better approximation than the other;[64] hence, the fit to the experimental data may be better for one method than the other. As aforementioned, the Friedman method is exact but taking a derivative (as is required in the method) introduces noise, which can lead to a lower value of R^2. It should be noted that the goodness of fit is not always a suitable criterion for deciding which methods are the best because it does not determine whether the activation energies are correct. The difference in the values of R^2 of the pyrolysis and copyrolysis experiments in Table 4 indicated that the rate of temperature increase (always assumed to be constant) may be less constant than in others or perhaps there may be an overlap of organic and inorganic loss temperature ranges. This phenomenon also occurred for oil shale.[66,67]

In Table 5, the values of the activation energy determined using the KAS, FWO, and Friedman methods for conversion rates from 0.1 to 0.3 increased because protein decomposition occurs in this conversion range (233−340 °C). The value of the activation energy at conversion rates of 0.4−0.6 indicated the amount of energy required to decompose cellulose (326−393 °C). Decomposition of lipids and lignin compounds required higher activation energy values (conversion rates of 0.6−0.9, temperature range of 377−484 °C). Similar to that found for the pyrolysis experiments, the activation energies of the copyrolysis of *B. braunii* and VBC based on the KAS (195.20 ± 17.40 kJ/mol) and FWO (195.60 ± 17.70 kJ/mol) methods were similar. In contrast, the activation energy calculated based on the Friedman method was higher (225.93 ± 20.70 kJ/mol). The comparison of the activation energies of the pyrolysis and copyrolysis experiments at different conversion rates calculated by the KAS, FWO, and Friedman methods is given in Figure 5.

The activation energy for the copyrolysis of *B. braunii* and VBC was higher than the activation energy for pyrolysis of *B. braunii* alone: the activation energy was affected by the composition of the sample mixture. In general, reactions with higher activation energy require higher reaction temperatures or longer reaction durations. Chen et al.[54] have found that the average activation energies based on the KAS and FWO methods of the copyrolysis of *Chlorella vulgaris* and coal (in ratios of 7:3 and 3:7) were higher than that of *C. vulgaris* pyrolysis alone. Furthermore, the copyrolysis of *Nannochloropsis* sp. and Colombian bituminous coal (in ratios of 1:1 and 1:4) required a higher activation energy than the pyrolysis of *Nannochloropsis* sp.[68] (Table 6). Thus, in general, there is a tendency that the addition of coal to microalgae may increase the activation energy of the thermal decomposition process of the mixture. However, it should be noted that this is not always the case and depends on the chemical and physical characteristics of the samples. For instance, when the ratio of *C. vulgaris* and coal was 5:5, the activation energy of the copyrolysis was lower than that of *C. vulgaris* pyrolysis.[54] Each species of microalgae contains different lipids, proteins, carbohydrates, and chlorophyll,[69−71] as well as different rank coals, which contain highly varied organic and mineral matter.[72] The differences in these chemical and physical

Table 6. Activation Energy (E_a) of Copyrolysis of Microalgae and Coal with Different Weight Ratios Based on the KAS and FWO Methods

algae/coal	weight ratio	activation energy (kJ/mol) KAS	activation energy (kJ/mol) FWO	references
B. braunii		183.95	185.15	this study
B. braunii/VBC	1:1	195.20	195.60	
C. vulgaris		335.69	329.51	54
C. vulgaris/semianthracite coal	3:7	416.01	421.19	
C. vulgaris/semianthracite coal	5:5	320.77	312.89	
C. vulgaris/semianthracite coal	7:3	407.57	397.05	
Nannochloropsis sp.		171.0	173.2	68
Nannochloropsis sp./Colombian bituminous coal	1:1	195.0	196.3	
Nannochloropsis sp./Colombian bituminous coal	1:4	266.8	265.4	

https://doi.org/10.1021/acsomega.1c04818
ACS Omega 2021, 6, 32032−32042

characteristics of the microalgae and coal samples will lead to different thermal decomposition temperatures and, thus, the activation energy of the pyrolysis and/or copyrolysis experiments of microalga and/or coal samples.[24,54,68]

3. CONCLUSIONS

The copyrolysis of the microalgae *B. braunii* and VBC decreased the temperature range of active pyrolysis relative to that of *B. braunii* pyrolysis alone. However, the thermal decomposition temperature at each conversion rate in the copyrolysis experiments increased due to differences in the chemical composition of the mixture, especially in VBC, which required higher temperatures for thermal decomposition to occur.

The pyrolysis of *B. braunii* and the copyrolysis of *B. braunii* and VBC consisted of three stages, each of which occurred over different temperature ranges. In the pyrolysis process, the first stage was the evaporation of water and volatile compounds, which occurred at around <±150 °C. The second stage was active pyrolysis in a temperature range of ±150−550 °C. The third stage was passive pyrolysis at ±550−800 °C. In the copyrolysis process, the first stage was the evaporation of water and volatile compounds (<±150 °C), the second stage was the active copyrolysis (±150−545 °C), and, finally, the decomposition stage (±545−800 °C).

Calculations of activation energy using the three isoconversional models (KAS, FWO, and Friedman) showed that the copyrolysis of *B. braunii* and VBC required more energy (higher E_a) than the pyrolysis of the microalgae themselves. However, it should be noted that the use of different ratios of microalgae and coals in copyrolysis is important for a better understanding of the effect of the composition of samples on the activation energy. It is also necessary to pay attention to the chemical composition of the resulting pyrolysis product, such as the composition of the aliphatic and aromatic compounds, if the desired product is used as a fuel.

4. MATERIALS AND METHODS

4.1. Materials and Sample Preparations. *B. braunii* was cultivated for 3 to 4 months at the Laboratory of Animal Physiology, Developmental and Molecular Animals, Faculty of Mathematics and Natural Sciences, Mulawarman University, Indonesia. The medium for microalgal cultivation (AF6) was prepared using the method reported by Kato.[73] A sample of *B. braunii* was taken from the fresh waters of Tenggarong, Kutai Kartanegara Regency, East Kalimantan, Indonesia. A plankton net with a mesh size of 100 μm was used to obtain *B. braunii* from the sampling location. For reference, the *B. braunii* isolate obtained was compared to *B. braunii* OIT 413 strain from the Osaka Institute of Technology, Osaka, Japan. The algal colonies were purified by dilution and inoculated into liquid medium AF6 in a 150 mL Erlenmeyer flask. The inoculum was incubated under 12L/12D artificial photoperiod conditions (light and dark hours) with a light intensity of 1.2 ± 0.2 flux at 25−27 °C. After 90 days, the cultures were harvested. The type of *B. braunii* was confirmed by the Nile red staining method and evaluated using a fluorescence microscope (Nikon Diaphot 504, Nikon Corporation, Japan).

For copyrolysis experiments and characterizations, the algal paste was centrifuged at 5000 rpm for 30 s to separate the algal sample and the supernatant. In the next stage, the algal samples were homogenized for 30 s at a speed of 300 rpm and dried using a freeze-drier for 24 h. The freeze-dried samples were stored at 20 °C. The procedure was repeated several times to obtain the required number of freeze-dried samples for the next steps (characterization and pyrolysis).

VBC, Loy Yang Low Ash, with a moisture content of 60 wt % (as received) and an ash content of 3.25% db (dry-basis),[74] was provided by Alan Chafee's Research Group, School of Chemistry, Monash University, Australia. The VBC was dried in an oven at 105 °C under a flow of N_2 to reduce its moisture content to 7.5% (similar to that of the microalgal sample). After that, the dried coal sample was mixed with the freeze-dried microalgae in a ratio of 1:1 (w/w) using a Micro Ball Mill before the copyrolysis experiments.

Nitrogen (N_2) and air for copyrolysis were provided by Air Liquide. All chemicals were used without further purification.

4.2. Characterization of *B. braunii*. *4.2.1. Water Content and Ash Content Analyses.* The water content and ash content were determined using a TGA Setaram TAG 16 simultaneous symmetrical thermo analyzer (Setaram, France). To determine the water content, 25 mg of the freeze-dried sample was heated in an alumina cup from room temperature to 110 °C and held for 15 min under a nitrogen gas at a flow rate of 140 mL/min. The water content was calculated as the percentage of mass loss from the sample at room temperature to 110 °C and based on duplicate experiments. To determine the ash content, 25 mg of the freeze-dried sample was heated in an alumina cup from room temperature to 800 °C and held for 90 min under air at a flow rate of 70 mL/min. The ash content was calculated as the percentage of mass loss from the sample between room temperature to 800 °C and based on duplicate experiments.

4.2.2. Protein Content Analysis. The protein content was determined by the fluorometric method using a Qubit 4 Fluorometer manufactured by Thermo Fisher Scientific, USA. Initially, 1 mg of the microalgal sample was dissolved in 1 mL of 1% NaCl solution. The working solution was prepared in a ratio of the 1:200 Qubit protein reagent in protein buffer. The composition of the working solution was 6 μL of the protein reagent and 1194 μL of Qubit buffer. At the standard solution preparation stage, 190 μL of the Qubit working solution was added to each of the three standard tubes. Then, 10 μL of standard Qubit was added to each tube and homogenized using a vortex for 2−3 s. As much as 10 μL of the microalgal sample was then inserted into the tube, and the working solution was added to the microalgal sample until the total volume of the mixture was 200 μL. The mixture was then homogenized using a vortex for 2−3 s. The sample solution was allowed to stand for 15 min before it was analyzed.

4.2.3. Lipid Test. Lipid analysis was carried out by extracting the *B. braunii* culture using ethanol in the ratio 4:1 mL/g at 27 °C for 30 min. After that, the solution was centrifuged at 4500 rpm for 10 min to separate the microalgal sample from the impurities. Hexane was then added to the sample and centrifuged to separate the hexane/lipid part from the water and ethanol. The lipids were stored at 4 °C prior to analysis. Lipid tests using an Agilent 7890B gas chromatograph (Agilent Intelligent GC Systems, USA) were carried out by the Food Nutrition Laboratory, Gadjah Mada University, Indonesia.

4.2.4. Analysis of Chlorophyll. Initially, 10 mL of microalgal paste was placed in a 15 mL vial, and the sample was centrifuged for 15 min at a speed of 3000 rpm. The solid fraction was kept, and the supernatant was discarded. The solid fraction was diluted in a 9:1 acetone solution (9 mL acetone/1

https://doi.org/10.1021/acsomega.1c04818
ACS Omega 2021, 6, 32032−32042

mL water). The mixture was mixed for 20 min at a speed of 5000 rpm with a vortex mixer and was analyzed with UV−vis spectrophotometry (SP-UV52N, Wincom Company Ltd., China). Analyses of chlorophyll *a*, *b*, and total chlorophyll were carried out at 663 and 646 nm. The total chlorophyll, chlorophyll *a*, and *b* were calculated based on eqs 1−3.[75]

$$\text{Total chlorophyll (mg/L)} = (17.3 \times A_{646}) + (7.18 \times A_{663}) \quad (1)$$

$$\text{Chlorophyll } a \text{ (mg/L)} = (12.21 \times A_{663}) - (2.81 \times A_{646}) \quad (2)$$

$$\text{Chlorophyll } b \text{ (mg/L)} = (20.13 \times A_{646}) - (5.03 \times A_{663}) \quad (3)$$

where A_{663} was the absorbance value at 663 nm and A_{646} was the absorbance value at 646 nm.

4.3. Copyrolysis Experiments. The kinetic study of *B. braunii* and VBC was carried out by TGA in nitrogen and air using a Setaram TAG 16 simultaneous symmetrical thermo analyzer (Setaram, France). A small amount of a 1:1 (w/w) mixture of *B. braunii* and VBC (10−20 mg) was put into an alumina cup. The sample was exposed to nitrogen (140 mL/min) for 10 min and then heated from room temperature to 850 °C at heating rates of 10, 15, 20, and 25 °C/min. The temperature was maintained for 20 min in the nitrogen gas stream; then, the nitrogen gas was changed to air at a flow rate of 70 mL/min at the same temperature for another 20 min. Next, the temperature was lowered to 20 °C at 20 °C/min in an air stream (70 mL/min). The temperature was maintained for 30 min. For comparison, the same pyrolysis procedure was performed on *B. braunii* samples at the same heating rates and VBC samples at a heating rate of 25 °C/min.

Based on the TG and dTG curves, the pyrolysis of *B. braunii* and the copyrolysis of *B. braunii* and VBC can be divided into three stages. The temperature ranges of the three stages were determined based on the dTG curves generated from experiments with different heating rates. The maximum temperature in the first stage is the temperature at which the first peak of the dTG curve has sloped (lowest dTG value). In contrast to the first stage, which comprises only one peak, the second stage on the dTG curve consists of several peaks. The temperature range in the second stage is the temperature after the first stage is completed to the temperature at which the peaks on the dTG curve have flattened. The initial temperature in the third stage is the temperature after the end of the second stage. The determination of the temperature ranges was similar to that reported by Chen et al.[54]

The data obtained were analyzed with three kinetic models, namely, KAS, FWO, and Friedman, to obtain the value of the activation energy. The conversion value (α) is the proportion of the volatile organic matter at a certain pyrolysis temperature (the amount of the organic matter lost divided by the total volatile organic matter). The conversion values used in this study were 0.1, 0.2, 0.3, 0.4, 0.5, 0.6, 0.7, 0.8, and 0.9.

The KAS method[40] is an integral isoconversional method based on eq 4

$$\ln\left(\frac{\beta}{T_\alpha^2}\right) = \text{const} - \frac{E_a}{RT_\alpha} \quad (4)$$

From the above equation, the activation energy value (E_a) can be calculated from the Cartesian slope plotted using $1/T_\alpha$ as the *x*-axis and $\ln(\beta/T_\alpha^2)$ as the *y*-axis. Here, T is the temperature (K), β is the heating rate (°C/min), and R is the universal gas constant (8.314 J K^{-1} mol^{-1}).

The FWO method[41] is an integral isoconversional method, based on eq 5

$$\ln \beta = -1.0516\frac{E_a}{RT_\alpha} + \text{const} \quad (5)$$

The activation energy (E_a) can be calculated from the Cartesian slope plotted using $1/T_\alpha$ as the *x*-axis and $\ln \beta$ as the *y*-axis. Here, T is the temperature (K), β is the heating rate (°C/min), and R is the universal gas constant (8.314 J K^{-1} mol^{-1}).

The Friedman method[42] is a differential isoconversional method, which is expressed as

$$\ln\left(\beta \frac{d\alpha}{dT}\right) = \text{const} - \frac{E_a}{RT_\alpha} \quad (6)$$

The activation energy value (E_a) can be calculated from the Cartesian slope plotting using $1/T_\alpha$ as the *x*-axis and $\ln\left(\beta \frac{d\alpha}{dT}\right)$ as the *y*-axis. Here, T is the temperature (K), β is the heating rate (°C/min), and R is the universal gas constant (8.314 J K^{-1} mol^{-1}).

AUTHOR INFORMATION

Corresponding Author

R. R. Dirgarini Julia Nurlianti Subagyono − *Chemistry Department, Mulawarman University, Samarinda 75119, Indonesia;* orcid.org/0000-0002-0098-6266; Email: dirgarini@fmipa.unmul.ac.id

Authors

Wardina Masdalifa − *Chemistry Department, Mulawarman University, Samarinda 75119, Indonesia*

Siti Aminah − *Chemistry Department, Mulawarman University, Samarinda 75119, Indonesia*

Rudy Agung Nugroho − *Biology Department and Research Center of Natural Products from Tropical Rainforest (PUI PT OKTAL), Mulawarman University, Samarinda 75119, Indonesia*

Mamun Mollah − *School of Chemistry, Monash University, Clayton, Victoria 3800, Australia*

Veliyana Londong Allo − *Chemistry Department, Mulawarman University, Samarinda 75119, Indonesia*

Rahmat Gunawan − *Chemistry Department, Mulawarman University, Samarinda 75119, Indonesia*

Complete contact information is available at: https://pubs.acs.org/10.1021/acsomega.1c04818

Notes

The authors declare no competing financial interest.

ACKNOWLEDGMENTS

We would like to acknowledge the Ministry of Research, Technology and Higher Education of the Republic of Indonesia for financial support in the project through the World Class Research Program (Contract number: 585/UN17.L1/PG/2021). We would like to thank Prof. Alan L. Chaffee from Monash University, Australia, for providing VBC samples and assistance with TGA analyses. We thank Rudianto, Stephanie Layuk and Widha Prahastika for their

assistance in preparing the algal sample and characterization of *Botryococcus braunii*.

REFERENCES

(1) Zhou, L.; Zhang, G.; Reinmöller, M.; Meyer, B. Effect of inherent mineral matter on the co-pyrolysis of highly reactive brown coal and wheat straw. *Fuel* **2019**, *239*, 1194−1203.
(2) Liu, Q.; Zhong, W.; Tang, R.; Yu, H.; Gu, J.; Zhou, G.; Yu, A. Experimental tests on co-firing coal and biomass waste fuels in a fluidised bed under oxy-fuel combustion. *Fuel* **2021**, *286*, 119312.
(3) Verma, M.; Loha, C.; Sinha, A. N.; Chatterjee, P. K. Drying of biomass for utilising in co-firing with coal and its impact on environment − A review. *Renewable Sustainable Energy Rev.* **2017**, *71*, 732−741.
(4) Wei, J.; Wang, M.; Wang, F.; Song, X.; Yu, G.; Liu, Y.; Vuthaluru, H.; Xu, J.; Xu, Y.; Zhang, H.; Zhang, S. A review on reactivity characteristics and synergy behavior of biomass and coal Co-gasification. *Int. J. Hydrogen Energy* **2021**, *46*, 17116−17132.
(5) Seçer, A.; Küçet, N.; Fakı, E.; Hasanoğlu, A. Comparison of co−gasification efficiencies of coal, lignocellulosic biomass and biomass hydrolysate for high yield hydrogen production. *Int. J. Hydrogen Energy* **2018**, *43*, 21269−21278.
(6) Rizkiana, J.; Guan, G.; Widayatno, W. B.; Hao, X.; Huang, W.; Tsutsumi, A.; Abudula, A. Effect of biomass type on the performance of cogasification of low rank coal with biomass at relatively low temperatures. *Fuel* **2014**, *134*, 414−419.
(7) Ismail, T. M.; Banks, S. W.; Yang, Y.; Yang, H.; Chen, Y.; Bridgwater, A. V.; Ramzy, K.; Abd El-Salam, M. Coal and biomass co-pyrolysis in a fluidized-bed reactor: Numerical assessment of fuel type and blending conditions. *Fuel* **2020**, *275*, 118004.
(8) Gouws, S. M.; Carrier, M.; Bunt, J. R.; Neomagus, H. W. J. P. Co-pyrolysis of coal and raw/torrefied biomass: A review on chemistry, kinetics and implementation. *Renewable Sustainable Energy Rev.* **2021**, *135*, 110189.
(9) Wu, Z.; Zhang, J.; Zhang, B.; Guo, W.; Yang, G.; Yang, B. Synergistic effects from co-pyrolysis of lignocellulosic biomass main component with low-rank coal: Online and offline analysis on products distribution and kinetic characteristics. *Appl. Energy* **2020**, *276*, 115461.
(10) Zhang, C.; Li, S.; Ouyang, S.; Tsang, C.-W.; Xiong, D.; Yang, K.; Zhou, Y.; Xiao, Y. Co-pyrolysis characteristics of *Camellia oleifera* shell and coal in a TGA and a fixed-bed reactor. *J. Anal. Appl. Pyrolysis* **2021**, *155*, 105035.
(11) Nyoni, B.; Duma, S.; Bolo, L.; Shabangu, S.; Hlangothi, S. P. Co-pyrolysis of South African bituminous coal and *Scenedesmus* microalgae: Kinetics and synergistic effects study. *Int. J. Coal Sci. Technol.* **2020**, *7*, 807−815.
(12) Chisti, Y. Biodiesel from microalgae. *Biotechnol. Adv.* **2007**, *25*, 294−306.
(13) Duan, P.; Savage, P. E. Hydrothermal liquefaction of a microalga with heterogeneous catalysts. *Ind. Eng. Chem. Res.* **2011**, *50*, 52−61.
(14) Huber, G. W.; Iborra, S.; Corma, A. Synthesis of transportation fuels from biomass:chemistry, catalysts, and engineering. *Chem. Rev.* **2006**, *106*, 4044−4098.
(15) Jena, U.; Das, K. C.; Kastner, J. R. Effect of operating conditions of thermochemical liquefaction on biocrude production from *Spirulina platensis*. *Bioresour. Technol.* **2011**, *102*, 6221−6229.
(16) Wijffels, R. H. Potential of sponges and microalgae for marine biotechnology. *Trends Biotechnol.* **2008**, *26*, 26−31.
(17) Al-Hothaly, K. A.; Adetutu, E. M.; Taha, M.; Fabbri, D.; Lorenzetti, C.; Conti, R.; May, B. H.; Shar, S. S.; Bayoumi, R. A.; Ball, A. S. Bio-harvesting and pyrolysis of the microalgae *Botryococcus braunii*. *Bioresour. Technol.* **2015**, *191*, 117−123.
(18) Piloni, R. V.; Daga, I. C.; Urcelay, C.; Moyano, E. L. Experimental investigation on fast pyrolysis of freshwater algae. Prospects for alternative bio-fuel production. *Algal Res.* **2021**, *54*, 102206.
(19) Ren, R.; Han, X.; Zhang, H.; Lin, H.; Zhao, J.; Zheng, Y.; Wang, H. High yield bio-oil production by hydrothermal liquefaction of a hydrocarbon-rich microalgae and biocrude upgrading. *Carbon Resour. Convers.* **2018**, *1*, 153−159.
(20) Banerjee, A.; Sharma, R.; Chisti, Y.; Banerjee, U. C. *Botryococcus braunii*: A Renewable Source of Hydrocarbons and Other Chemicals. *Crit. Rev. Biotechnol.* **2002**, *22*, 245−279.
(21) Gouveia, L.; Oliveira, A. C. Microalgae as a raw material for biofuels production. *J. Ind. Microbiol. Biotechnol.* **2009**, *36*, 269−274.
(22) Metzger, P.; Largeau, C. *Botryococcus braunii*: a rich source for hydrocarbons and related ether lipids. *Appl. Microbiol. Biotechnol.* **2005**, *66*, 486−496.
(23) Hayashi, J.-i.; Li, C.-Z. Structure and Properties of Victorian Brown Coal. In *Advances in the Science of Victorian Brown Coal*; Li, C.-Z., Ed.; Elsevier Science: Amsterdam, 2004; Chapter 2, pp 11−84.
(24) Wu, Z.; Yang, W.; Tian, X.; Yang, B. Synergistic effects from co-pyrolysis of low-rank coal and model components of microalgae biomass. *Energy Convers. Manage.* **2017**, *135*, 212−225.
(25) Liu, Y.-Q.; Lim, L. R. X.; Wang, J.; Yan, R.; Mahakhant, A. Investigation on Pyrolysis of Microalgae *Botryococcus braunii* and Hapalosiphon sp. *Ind. Eng. Chem. Res.* **2012**, *51*, 10320−10326.
(26) Mollah, M. M.; Jackson, W. R.; Marshall, M.; Chaffee, A. L. An attempt to produce blast furnace coke from Victorian brown coal. *Fuel* **2015**, *148*, 104−111.
(27) Kirtania, K.; Bhattacharya, S. Pyrolysis kinetics and reactivity of algae−coal blends. *Biomass Bioenergy* **2013**, *55*, 291−298.
(28) Azizi, K.; Keshavarz Moraveji, M.; Abedini Najafabadi, H. Characteristics and kinetics study of simultaneous pyrolysis of microalgae *Chlorella vulgaris*, wood and polypropylene through TGA. *Bioresour. Technol.* **2017**, *243*, 481−491.
(29) Anca-Couce, A.; Tsekos, C.; Retschitzegger, S.; Zimbardi, F.; Funke, A.; Banks, S.; Kraia, T.; Marques, P.; Scharler, R.; de Jong, W.; Kienzl, N. Biomass pyrolysis TGA assessment with an international round robin. *Fuel* **2020**, *276*, 118002.
(30) Mishra, R. K.; Mohanty, K. Kinetic analysis and pyrolysis behaviour of waste biomass towards its bioenergy potential. *Bioresour. Technol.* **2020**, *311*, 123480.
(31) Hameed, S.; Sharma, A.; Pareek, V.; Wu, H.; Yu, Y. A review on biomass pyrolysis models: Kinetic, network and mechanistic models. *Biomass Bioenergy* **2019**, *123*, 104−122.
(32) Varma, A. K.; Mondal, P. Physicochemical characterization and pyrolysis kinetics of wood sawdust. *Energy Sources, Part A* **2016**, *38*, 2536−2544.
(33) Li, J.; Qiao, Y.; Zong, P.; Wang, C.; Tian, Y.; Qin, S. Thermogravimetric Analysis and Isoconversional Kinetic Study of Biomass Pyrolysis Derived from Land, Coastal Zone, and Marine. *Energy Fuels* **2019**, *33*, 3299−3310.
(34) Naqvi, S. R.; Naqvi, M.; Noor, T.; Hussain, A.; Iqbal, N.; Uemura, Y.; Nishiyama, N. Catalytic Pyrolysis Of *Botryococcus braunii* (microalgae) Over Layered and Delaminated Zeolites For Aromatic Hydrocarbon Production. *Energy Procedia* **2017**, *142*, 381−385.
(35) Heydari, M.; Rahman, M.; Gupta, R. Kinetic Study and Thermal Decomposition Behavior of Lignite Coal. *Int. J. Chem. Eng.* **2015**, *2015*, 481739.
(36) Soria-Verdugo, A.; Morgano, M. T.; Mätzing, H.; Goos, E.; Leibold, H.; Merz, D.; Riedel, U.; Stapf, D. Comparison of wood pyrolysis kinetic data derived from thermogravimetric experiments by model-fitting and model-free methods. *Energy Convers. Manage.* **2020**, *212*, 112818.
(37) Šimon, P. Isoconversional methods. *J. Therm. Anal. Calorim.* **2004**, *76*, 123.
(38) Ali, I.; Naqvi, S. R.; Bahadar, A. Kinetic analysis of *Botryococcus braunii* pyrolysis using model-free and model fitting methods. *Fuel* **2018**, *214*, 369−380.
(39) Arbeláez, A. A.; Giraldo, N. D.; Pérez, J. F.; Atehortúa, L. Pyrolysis Kinetics Using TGA and Simulation of Gasification of the Microalga *Botryococcus braunii*. *BioEnergy Res.* **2019**, *12*, 1077−1089.

https://doi.org/10.1021/acsomega.1c04818
ACS Omega 2021, 6, 32032−32042

(40) Akahira, T.; Sunose, T. Method of determining activation deterioration constant of electrical insulating materials. *Res. Rep. Chiba Inst. Technol.* **1971**, *16*, 22−31.
(41) Flynn, J. H.; Wall, L. A. General treatment of the thermogravimetry of polymers. *J. Res. Natl. Bur. Stand., Sect. A* **1966**, *70*, 487−523.
(42) Friedman, H. L. Kinetics of thermal degradation of char-forming plastics from thermogravimetry. Application to a phenolic plastic. *J. Polym. Sci., Part C: Polym. Symp.* **1964**, *6*, 183−195.
(43) Al-Ayed, O. S. Study of the Kinetics and Mechanisms of Thermal Decomposition of Ellajjun Oil Shale. *The Sixth Jordan International Chemical Engineering Conference (JIChEC06), Jordan, 2012*: Jordan, 2012; p 12.
(44) Gogoi, M.; Konwar, K.; Bhuyan, N.; Borah, R. C.; Kalita, A. C.; Nath, H. P.; Saikia, N. Assessments of pyrolysis kinetics and mechanisms of biomass residues using thermogravimetry. *Bioresour. Technol. Rep.* **2018**, *4*, 40−49.
(45) Obernberger, I.; Thek, G. Physical characterisation and chemical composition of densified biomass fuels with regard to their combustion behaviour. *Biomass Bioenergy* **2004**, *27*, 653−669.
(46) Li, C.-Z.; Tan, L. L. Formation of NO_x and SO_x precursors during the pyrolysis of coal and biomass. Part III. Further discussion on the formation of HCN and NH_3 during pyrolysis. *Fuel* **2000**, *79*, 1899−1906.
(47) Nussbaumer, T. Combustion and Co-combustion of Biomass:Fundamentals ,Technologies ,and Primary Measures for Emission Reduction. *Energy Fuels* **2003**, *17*, 1510−1521.
(48) Subagyono, D. J. N.; Marshall, M.; Jackson, W. R.; Chow, M.; Chaffee, A. L. Reactions with CO/H_2O of two marine algae and comparison with reactions under H_2 and N_2. *Energy Fuels* **2014**, *28*, 3143−3156.
(49) Simoneit, B. R. T.; Rushdi, A. I.; bin Abas, M. R.; Didyk, B. M. Alkyl amides and nitriles as novel tracers for biomass burning. *J. Environ. Sci. Technol.* **2002**, *37*, 16−21.
(50) Furimsky, E. Catalytic hydrodeoxygenation. *Appl. Catal., A* **2000**, *199*, 147−190.
(51) Sau, M.; Basak, K.; Manna, U.; Santra, M.; Verma, R. P. Effects of organic nitrogen compounds on hydrotreating and hydrocracking reactions. *Catal. Today* **2005**, *109*, 112−119.
(52) Jamilatun, S.; Budhijanto, B.; Rochmadi, R.; Budiman, A. Thermal Decomposition and Kinetic Studies of Pyrolysis of *Spirulina platensis* Residue. *Int. J. Renewable Energy Dev.* **2017**, *6*, 193.
(53) Rudra, S. G.; Singh, H.; Basu, S.; Shivhare, U. S. Enthalpy entropy compensation during thermal degradation of chlorophyll in mint and coriander puree. *J. Food Eng.* **2008**, *86*, 379−387.
(54) Chen, C.; Ma, X.; He, Y. Co-pyrolysis characteristics of microalgae *Chlorella vulgaris* and coal through TGA. *Bioresour. Technol.* **2012**, *117*, 264−273.
(55) Agrawal, A.; Chakraborty, S. A kinetic study of pyrolysis and combustion of microalgae *Chlorella vulgaris* using thermo-gravimetric analysis. *Bioresour. Technol.* **2013**, *128*, 72−80.
(56) Brebu, M.; Vasile, C. Thermal degradation of lignin-A review. *Cellul. Chem. Technol.* **2010**, *44*, 353−363.
(57) Chen, X.; Liu, L.; Zhang, L.; Zhao, Y.; Qiu, P. Pyrolysis Characteristics and Kinetics of Coal−Biomass Blends during Co-Pyrolysis. *Energy Fuels* **2019**, *33*, 1267−1278.
(58) Qi, Y.; Hann, W.; Subagyono, D. J. N.; Fei, Y.; Marshall, M.; Jackson, W. R.; Patti, A. F.; Chaffee, A. L. Characterisation of the products of low temperature pyrolysis of Victorian brown coal in a semi-continuous/flow through system. *Fuel* **2018**, *234*, 1422−1430.
(59) Hayatsu, R.; Botto, R. E.; Scott, R. G.; McBeth, R. L.; Winans, R. E. Evaluation of lignin and cellulose contributions to low-rank coal formation by alkaline cupric oxide oxidation. *Fuel* **1986**, *65*, 821−826.
(60) Mishra, R. K.; Mohanty, K. Pyrolysis kinetics and thermal behavior of waste sawdust biomass using thermogravimetric analysis. *Bioresour. Technol.* **2018**, *251*, 63−74.
(61) Kaur, R.; Gera, P.; Jha, M. K.; Bhaskar, T. Pyrolysis kinetics and thermodynamic parameters of castor (*Ricinus communis*) residue using thermogravimetric analysis. *Bioresour. Technol.* **2018**, *250*, 422−428.
(62) Ceylan, S.; Topcu, Y.; Ceylan, Z. Thermal behaviour and kinetics of alga Polysiphonia elongata biomass during pyrolysis. *Bioresour. Technol.* **2014**, *171*, 193−198.
(63) Yao, Z.; Yu, S.; Su, W.; Wu, W.; Tang, J.; Qi, W. Kinetic studies on the pyrolysis of plastic waste using a combination of model-fitting and model-free methods. *Waste Manage. Res.* **2020**, *38*, 77−85.
(64) Vyazovkin, S.; Burnham, A. K.; Favergeon, L.; Koga, N.; Moukhina, E.; Pérez-Maqueda, L. A.; Sbirrazzuoli, N. ICTAC Kinetics Committee recommendations for analysis of multi-step kinetics. *Thermochim. Acta* **2020**, *689*, 178597.
(65) Huidobro, J. A.; Iglesias, I.; Alfonso, B. F.; Espina, A.; Trobajo, C.; Garcia, J. R. Reducing the effects of noise in the calculation of activation energy by the Friedman method. *Chemom. Intell. Lab. Syst.* **2016**, *151*, 146−152.
(66) Amer, M. W.; Marshall, M.; Fei, Y.; Jackson, W. R.; Gorbaty, M. L.; Cassidy, P. J.; Chaffee, A. L. A comparison of the structure and reactivity of five Jordanian oil shales from different locations. *Fuel* **2014**, *119*, 313−322.
(67) Amer, M. W.; Marshall, M.; Fei, Y.; Roy Jackson, W.; Gorbaty, M. L.; Cassidy, P. J.; Chaffee, A. L. The structure and reactivity of a low-sulfur lacustrine oil shale (Colorado U.S.A.) compared with those of a high-sulfur marine oil shale (Julia Creek, Queensland, Australia). *Fuel Process. Technol.* **2015**, *135*, 91−98.
(68) Fermoso, J.; Corbet, T.; Ferrara, F.; Pettinau, A.; Maggio, E.; Sanna, A. Synergistic effects during the co-pyrolysis and co-gasification of high volatile bituminous coal with microalgae. *Energy Convers. Manage.* **2018**, *164*, 399−409.
(69) Wild, K. J.; Trautmann, A.; Katzenmeyer, M.; Steingaß, H.; Posten, C.; Rodehutscord, M. Chemical composition and nutritional characteristics for ruminants of the microalgae *Chlorella vulgaris* obtained using different cultivation conditions. *Algal Res.* **2019**, *38*, 101385.
(70) Prathima, A.; Karthikeyan, S. Characteristics of micro-algal biofuel from *Botryococcus braunii*. *Energy Sources, Part A* **2017**, *39*, 206−212.
(71) Brown, T. M.; Duan, P.; Savage, P. E. Hydrothermal Liquefaction and Gasification of *Nannochloropsis* sp. *Energy Fuels* **2010**, *24*, 3639−3646.
(72) Flores, R. M. Coal Composition and Reservoir Characterization. In *Coal and Coalbed Gas*; Flores, R. M., Ed.; Elsevier: Boston, 2014; Chapter 5, pp 235−299.
(73) Kato, S. Laboratory culture and morphology of *Colacium vesiculosum* Ehrb. (Euglenophyceae). *Jpn. J. Phycol.* **1982**, *30*, 63−67.
(74) Mollah, M. M.; Marshall, M.; Jackson, W. R.; Chaffee, A. L. Attempts to produce blast furnace coke from Victorian brown coal. 2. Hot briquetting, air curing and higher carbonization temperature. *Fuel* **2016**, *173*, 268−276.
(75) Harborne, A. J. *Phytochemical Methods: A Guide to Modern Techniques of Plant Analysis*; Springer Netherlands: 1998; p 302.

https://doi.org/10.1021/acsomega.1c04818
ACS Omega 2021, 6, 32032−32042